17th Brazilian Congress of Thermal Sciences and Engineering
November 25th-28th, 2018, Águas de Lindóia, SP, Brazil

ENCIT-2018-0480
NUMERICAL SIMULATION OF THE DROPLET BREAKUP WITH PERMANENT OBSTRUCTION IN MICROFLUIDIC T-JUNCTION

Angel Edecio Malaguera Mora
Ana Lúcia Fernandes de Lima e Silva
Sandro Metrevelle Marcondes de Lima e Silva
Bruno de Campos Salles Anselmo

Universidade Federal de Itajubá, Instituto de Engenharia Mecânica – IEM, Laboratório de Transferência de Calor – LabTC, Campus Prof. José Rodrigues Seabra, Av. BPS, 1303, Bairro Pinheirinho, Itajubá – MG, CEP 37500-903
aemalagueram@gmail.com, alfsilva@unifei.edu.br, metrevel@unifei.edu.br, brunocsa@gmail.com

Abstract. *The mechanisms of droplet breakup in a Microfluidic T-junction are mainly influenced by the capillary number* ($\boldsymbol{Ca}$) *and the ratio between the length of the droplet and the transverse dimension of the microchannel* ($\boldsymbol{l_o/w}$). *This work presents numerical simulations of an isolated liquid Taylor drop within a rectangular microchannel with T-junction in the range of capillary numbers of 0.0096 to 0.0904 and viscosity ratio of the dispersed and continuous phases of* $\boldsymbol{\mu_d/\mu_c = 0.125}$. *The numerical simulations were carried out with OpenFOAM 2.4 code by using the S-CLSVOF methodology which was implemented for this study. The use of S-CLSVOF and controlling time step and mesh resolution were able to increase the accuracy of capturing the interface dynamics. The results showed that the mechanisms of a droplet breakup inside a T junction are in a good agreement with literature.*

Keywords: *Microfluidic, OpenFOAM, T-junction, S-CLSVOF*

1. INTRODUCTION

The technology of two-phase flows in microfluids has recently advanced as a new field of research with application in processes involving chemical reactions, mixtures, emulsions, extractions and synthesis of medicines and materials. Bubbles and droplets are common in these applications and can be generated and/or manipulated in a controllable manner by dispersed and continuous flows with different geometries in microscale (Fu et al., 2011). T-shaped junction is a geometry frequently used for the production of droplets. The production of emulsions in microfluidic systems is an example of the application of devices to obtain particles on a micro-scale.

The dynamic behavior of the droplets within microchannels is complex, and the mechanisms of rupture through T-junctions depend on variables such as droplet length, flow velocity (dispersed and continuous), fluid properties and microchannel size. With low capillary numbers the forces deform the interface and generate a somewhat complex physics.

Numerical simulations of two-phase flows in very small geometries are well known to be complex. Large capillary forces, combined with the effect of the confinement, takes to the breakup of drops and the mechanisms that cause separation are just a few examples of the complexity of this kind of simulation (Afkhami et al. 2011). The calculation of physical properties through the interface, such as density and viscosity is another difficulty encountered. A good representation of the interface implies a more accurate calculation of these properties. There are various techniques designed in order to overcome these drawbacks. One of the most popular techniques are the methods based on meshes with capture or tracking interface. Among them can be mentioned Front Tracking methods, Immersed Boundary, Volume of Fluid (VOF) and Level Set (LS) and more recently the VOF-LS coupling (S-CLSVOF).

In this work, we present a three-dimensional numerical study of the dynamic behavior of a Taylor drop flowing through a microchannel with a T-junction. For this study, the S-CLSVOF methodology was implemented in OpenFOAM 2.4 (Greenshields, 2015). The drop behavior is influenced by surface tension, inlet velocities, and viscosity on the bubble length, shape, velocity, and film thickness around the drop. The aim of the present work was obtain data about the flow dynamics, the breakup conditions at the junction and the influence of numerical procedures such as mesh refinement, forces calculation and parasitic currents on the final results. The results were compared with experimental and numerical results from literature.

2. MATHEMATICAL FORMULATION

In this work, we study the dynamics of a drop flowing into a liquid within a microchannel T-junction. Both the dispersed phase (droplet) and the continuous phase (liquid) are treated as incompressible fluids. Physical properties such as density and viscosity are constant in each phase, varying only on the interface. In the microfluidic T-junction, the

surface tension effects are dominant. In this paper, the surface tension of fluid interface is regarded as the source term of Navier–Stokes equation. The Navier-Stokes equations in their conservative form can be written as follows:

$$\frac{\partial \rho}{\partial t} + \boldsymbol{\nabla}.(\rho \boldsymbol{u}) = 0 \tag{1}$$

$$\frac{\partial \rho \mathbf{u}}{\partial t} + \boldsymbol{\nabla}.(\rho \mathbf{u}\mathbf{u}) = -\boldsymbol{\nabla} p + \boldsymbol{\nabla}.\boldsymbol{\tau} + \rho \boldsymbol{g} + \boldsymbol{F}_s \tag{2}$$

where ρ is the density of the fluid, $\mathbf{u}$ is the velocity vector, t is the time, p the pressure, $\boldsymbol{\tau}$ the viscous stress tensor and $\boldsymbol{g}$ the gravity vector. $\boldsymbol{F}_s$ is the surface tension force per volume unit, acting on the interface between the two fluids and calculated by the continuum surface force CSF) model, described in section 2.1.

The equations of momentum are complemented by an equation relating the deformations and stresses in the fluid. In this study the fluids obey Newton's law of viscosity; the viscous stress tensor being given by:

$$\boldsymbol{\tau} = \mu(\boldsymbol{\nabla}\mathbf{u} + \boldsymbol{\nabla}\mathbf{u}^T) \tag{3}$$

where μ is the dynamic viscosity.

2.1 Coupled VOF with LS (S-CLSVOF)

In the Volume of Fluid method, the volume fraction is used as an indicator function (phase α) to mark the different fluids. The interface is defined as a transition region and is treated as a mixture of two fluids on each side of the interface. The volumetric fraction is defined as:

$$\alpha = \begin{cases} 1 \\ 0 < \alpha < 1 \\ 0 \end{cases} \tag{4}$$

Using this definition of volumetric fraction, we can represent the density and the viscosity as:

$$\rho(\boldsymbol{x}, t) = \alpha \rho_d + (1 - \alpha)\rho_c \tag{5}$$

$$\mu(\boldsymbol{x}, t) = \alpha \mu_d + (1 - \alpha)\mu_c \tag{6}$$

where the indices *d* and *c* represent the dispersed and continuous phase, respectively.

OpenFOAM uses an algebraic approach based on the counter-gradient transport to advect the volume fraction α. This scheme adds a compressive term to the α advection equation in order to retain the conservativeness, convergence, and boundedness (Albadawi et al., 2013). The advection equation is re-formulated as:

$$\frac{\partial(\alpha)}{\partial t} + \boldsymbol{\nabla}.(\mathbf{u}\alpha) + \boldsymbol{\nabla}.\big(\mathbf{u}_r \propto (1{-}\propto)\big) = 0 \tag{7}$$

where $\mathbf{u}_r = \mathbf{u}_d - \mathbf{u}_c$ is the relative velocity vector, referred to as the "compression velocity" of the interface. This additional term has the role of "compressing" the free surface towards a sharper one (it should be noted that the term compression is only a denotation and does not refer to the compressible flow). In addition, a scalar control parameter, c_α, is used to define the compression rate extension as:

$$\mathbf{u}_r = min\big(C_\alpha |\mathbf{u}|, max(|\mathbf{u}|)\big)\frac{\boldsymbol{\nabla}\alpha}{|\boldsymbol{\nabla}\alpha|} \tag{8}$$

C_α is generally chosen from 0 to 4 (Hoang et al., 2013), with a recommended value of 1. All the computational results presented here were obtained with a compression factor $C_\alpha = 1$. The influence of other values of the compression factor on the interface were already analyzed in the first preliminary results presented in this summary.

The traditional VOF has the advantage of an accurate mass conservation and the LS method provide an exact representation of the interface. The main objective of this work is the implementation the S-CLSVOF methodology in OpenFOAM using the algorithm implemented by Albadawi et al. (2013) for the simulation of bubbles rising in liquids. In this implementation of the Level Set function, the field ϕ is set where the position of the interface is defined by an iso-

line $\phi = 0$. Initially, the advection equation VOF is solved instead of the two advection equations VOF and LS, as done in the coupled method of Sussman and Puckett (2000).

The first step of the coupling is to assign an initial value to the LS function using the volume fraction function α and assuming that the position of the interface is defined in the contour of the iso-line where $\alpha = 0.5$:

$$\phi_0 = (2\alpha - 1).\Gamma \tag{9}$$

where Γ is a dimensionless number that depends on the size of the mesh Δx. According to Albadawi et al. (2013) the value of $\Gamma = 0.75\,\Delta x$ is adopted. The main criterion in choosing this value is related to a mesh size that produces less distortion in the interface during the breakup.

In Equation (16), the initial function ϕ_0 has a positive value in the dispersed phase and a negative value in the continuous phase. This value ϕ_0 is recalculated by solving the re-initialization equation:

$$\begin{cases} \phi(\mathbf{x}, 0) = \phi_0(\mathbf{x}) \\ \frac{\partial \phi}{\partial \tau} = S(\phi_0)(1 - |\nabla \phi|) \end{cases} \tag{10}$$

where τ is the artificial time, $\mathbf{x}$ is the position vector and $S(\phi_0)$ is a signal function. The solution converges when $|\nabla \phi| = 1$. The artificial time step was chosen as $\Delta\tau = 0.1\Delta x$, so that there are no abrupt changes in the LS function during the re-initialization.

In the reset equation (Eq. 10) some iterations are necessary (ϕ_{corr}). The number of iterations (ϕ_{corr}) is found according to the following condition for the chosen values of Γ and $\Delta\tau$:

$$\phi_{corr} = \frac{\epsilon}{\Delta\tau} \tag{11}$$

where ϵ is the interface thickness which defines the number of cells used for the transition of both fluids; $2\epsilon = 3\Delta x$ was used (Albadawi et al., 2013), where Δx is the mesh size.

The normal vector interface is defined as: $\mathbf{n} = \nabla\phi/|\nabla\phi|$. Thus, it provides a more precise and smooth interface curvature, $k = \nabla . \mathbf{n}$.

The surface tension force in the VOF-LS coupling can then be calculated as:

$$\mathbf{F}_S = \sigma k(\phi)\delta(\phi)\nabla\phi \tag{12}$$

where δ is the Dirac Delta function, used to limit the influence of surface tension to a narrow region in the interface. Function $\delta(\phi)$ is centered in the interface and is equal to zero in both fluids. It is defined as:

$$\delta(\phi) = \begin{cases} 0 & se\ |\phi| > \epsilon \\ \frac{1}{2\epsilon}\left(1 + cos\left(\frac{\pi\phi}{\epsilon}\right)\right) & se\ |\phi| \leq \epsilon \end{cases} \tag{13}$$

The physical properties on each cell can be defined as in the VOF method and calculated by using a Heaviside function (H) such as:

$$\rho(\phi) = \rho_d + (\rho_c - \rho_d)H \tag{14}$$

$$\mu(\phi) = \mu_d + (\mu_c - \mu_d)H \tag{15}$$

$$\text{where, } H(\phi) = \begin{cases} 0 & se\ \phi < -\epsilon \\ \frac{1}{2}\left[1 + \frac{\phi}{\epsilon} + \frac{1}{\pi} sen\left(\frac{\pi\phi}{\epsilon}\right)\right] & se|\phi| \leq \epsilon \\ 1 & se\ \ \phi > \epsilon \end{cases} \tag{16}$$

Equations (14) and (15) provide a smoother transition of properties through the interface (Albadawi et al., 2013).

3. NUMERICAL METHODOLOGY

OpenFOAM was chosen to be used in this work because besides being free license software, it is also an open source code that allows the user to make new implementations if necessary. In addition, it is a robust code and provides quite reliable results for a range of practical problems.

The basic mesh was generated with hexahedral cells using *blockMeshDict* utility, initially generating 1728000 computational cells. It was necessary to refine the mesh near the walls of the microchannel, in order to capture the thin layer of liquid between the drop and the wall, and thus correctly simulate the thickness of this lubricating film. For this, the *snappyHexMesh* tool was used allowing different levels of refinement in any zone of the domain as shown in Figure 1. It is observed that there is a greater refinement in the corners and in x direction, with the intention of capturing in detail the dynamics of the drop breakup, which occurs in this region. The local refinement adds approximately 2000000 computational cells to the basic mesh.

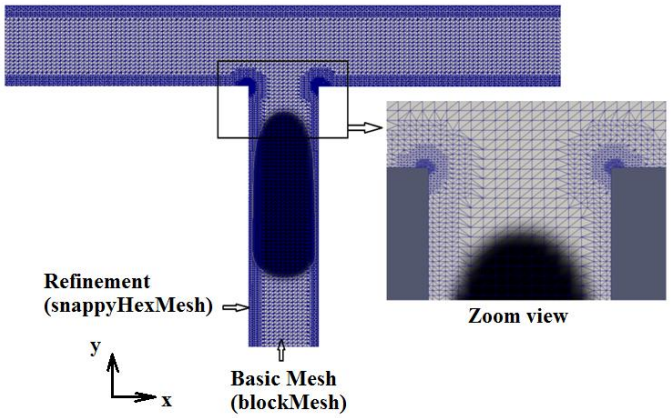

Figure 1**.** Computational unstructured grid generated with *blockMeshDict* and the *snappyHexMesh* tools.

In all simulations, a velocity of 0.04 m/s is imposed for the dispersed phase (drop) and for the continuous phase the velocity is in a range of 0.005 m/s and 0.035 m/s. The Neumann's condition is used for velocity at the two outlets. On the walls of the microchannel, the no-slip condition was imposed. The pressure at the domain inlet and outlet is unknown, and a threshold value is extrapolated from the inside of the flow. However, in both regions, the pressure gradients are small and it is enough to apply Neumann's condition (Favero, 2009) or type zeroGradient. Neumann's condition is also used in both the inlet and outlets of the computational domain for function ϕ.

The PIMPLE algorithm is applied to the pressure-velocity coupling, which is a variation of the PISO algorithm, allowing explicit relaxation of variables and implicit equations (Fiates, 2015). The temporal terms are discretized using a Cranck-Nicolson scheme, controlling the time step with a maximum Courant number equal to 0.2. At this point, it is important to report that high Courant numbers cause interface distortion due to increased parasitic currents (Hoang et al., 2013). In Section 4, the results of the simulations of a case comparing the effect of the Courant number are presented.

4. PRELIMINARY RESULTS

Simulations were performed for 3 values of the compression factor (Eq. 11), $C_\alpha = 1, 2$ and 3. In Figure 2, comparisons of the drop shape for $Ca = 0.0813$ and $l_0/w = 2.04$ are presented.

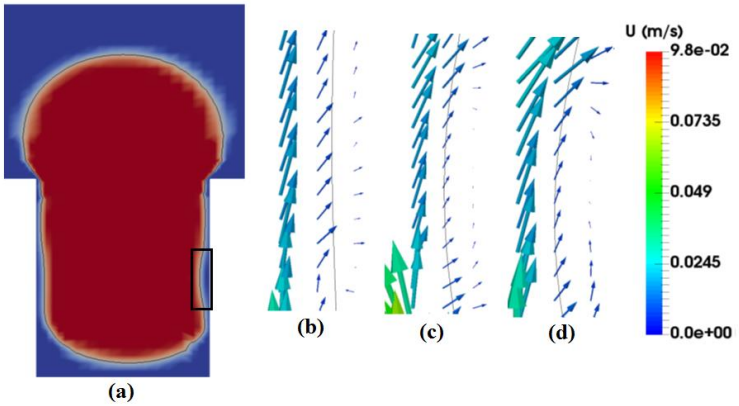

Figure 2. (a) Shape of the drop interface for $C_\alpha = 3$. Zoom view of a small region of the interface area for: (b) $C_\alpha = 1$, (c) $C_\alpha = 2$ and (d) $C_\alpha = 3$. Vectors are colored by the velocity magnitude.

The highlighted rectangle in Figure 2a, shows a bulging on the interface for $C_\alpha = 3$ also presented for $C_\alpha = 2$. In Figures 2c and 2d is possible to observe the development of small recirculations (parasitic currents) specially for $C_\alpha = 3$ that are not presented in Fig. 2b where the distortions are diminished. Parasitic currents is limited both by the terms of inertia and by the viscous term of the Navier-Stokes equations, which makes controlling or eliminating them a difficult task. Abrupt changes are found in the velocity field in that zone for $C_\alpha = 2$ and $C_\alpha = 3$ and they affect the form of the interface. In this way, the use of high values of this parameter generates non-physical velocities on the interface for the studied cases. On the other hand the compression factor did not affect the rupture mechanism in the tests performed. Therefore, the unit value was used for all simulations.

One of the difficulties in the simulation of droplets in microchannel is the fact that the parasitic currents also appears for small values of capillary numbers (0.0096 to 0.0904). The parasitic currents are unphysical movements of fluid generated by using models such as CSF techniques to approximate the calculation of surface tension on the interface (Renardy and Renardy, 2002). Its magnitude generally increases with surface tension and can become so large that it affects the prediction of the velocity field or, in extreme circumstances, can cause complete non-physical breakup of the interface. These spurious currents increase with the inverse of the capillary number but can be reduced in magnitude with greater refinement of the mesh or decreasing the time step. In this work, the parasitic currents were also controlled by defining a maximum Courant number in each simulation. In Figure 3, time evolution for the velocity field at junction is shown for *Ca = 0.0424 and lo/w = 1.8975* during the drop breakup. Four instants of time and Courant numbers of 0.2 and 0.5 are presented. In case of *Co = 0.2* (Fig. 3a), the rupture occurs at t = 0.095 s, whereas for *Co = 0.5* (Fig. 3b), the rupture occurs asymmetrically after t = 0.09625 s.

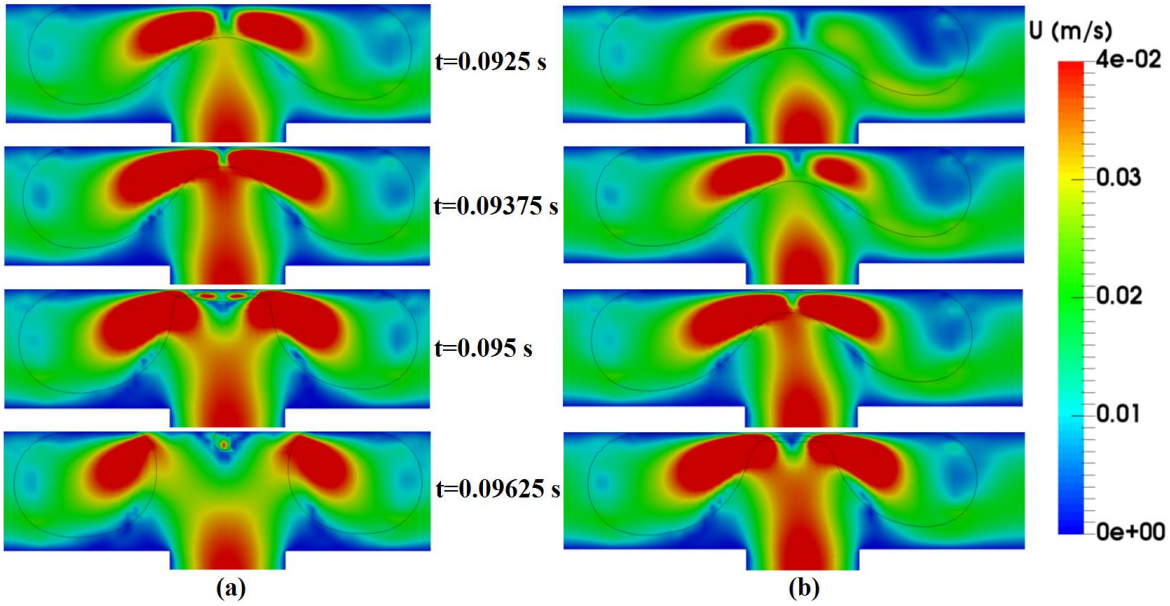

Figure 3. Time evolution of the velocity for *Ca = 0.0424*, *lo/w = 1.8975* and (a) Co = 0.2 and (b) Co = 0.5 in four instants of time during the droplet breakup.

5. CONCLUSIONS

Preliminary simulations of the droplet dynamics were performed in a T-junction microchannel with the S-CLSVOF methodology, which was implemented in OpenFOAM. The refinement of the computational domain near the wall and in the junction area was able to model the thin liquid layer between the droplet and the wall, thus avoiding that the same touch the wall.

It was verified that in the range of small capillary numbers investigated in this work ($0.0096 \leq Ca \leq 0.0904$) appear the parasitic currents tend to change influence the rupture mechanism as well as deforming the droplet in a non-physical way. These parasitic currents were contracted using a suitable Courant number

These preliminary simulations were performed in a microchannel of constant rectangular section and the properties of the fluids were also constant. Future simulations are aimed at studying the droplet breakup with partly obstruction, analyzing pressure fields, current lines and comparing the results with the consulted bibliography

6. ACKNOWLEDGEMENTS

The authors would like to thank CAPES for the doctoral scholarship and CNPq and FAPEMIG (TEC-APQ-00893-17) for the financial support. This work has made use of the computing facilities available at the Laboratory of

Computational Astrophysics of the Federal University of Itajubá (LAC-UNIFEI). The LAC-UNIFEI is maintained with grants from CAPES, CNPq and FAPEMIG.

7. REFERENCES

Afkhami, S., Leshansky, A. M. and Renardy, Y., 2011. "Numerical investigation of elongated drops in a microfluidic T-junction", *Physics of fluids*, 23, 022002 p. 1-14.

Albadawi, A., Donoghue, D. B., Robinson, A. J., Murray, D. B. and Delauré, Y. M. C., 2013. "Influence of surface tension implementation in Volume of Fluid and coupled Volume of Fluid with Level Set methods for bubble growth and detachment", *International Journal of Multiphase*, Flow, 53, p. 11-28.

Favero, J. L., 2009. *Simulação de escoamentos viscoelásticos: desenvolvimento de uma metodologia de análise utilizando o software OpenFOAM e equações constitutivas diferenciais*. Dissertação de Mestrado, Universidade Federal do Rio Grande do Sul. Porto Alegre, RS.

Fiates, J., 2015, *Desenvolvimento de uma metodologia para simulação de dispersão de gás inflamável por meio de CFD utilizando OpenFoam.* Dissertação de mestrado, Universidade Estadual de Campinas, Campinas.

Fu, T., Ma, Y., Funfschilling, D. and Huai, Z. L., 2011. "Dynamics of bubble breakup in a microfluidic T-junction divergence", *Chemical Engineering Science*, 66, p. 4184-4195.

Greenshields, C. J. 2015. *OpenFOAM User Guide Version 2.4.0 [PDF]*. OpenFOAM Foundation Ltd., 2015. Licensed under a Creative Commons Attribution-NonCommercial-NoDerivs 3.0 Unported License.

Hoang, D. A., Van Steijn, V., Portela, L. M., Kreutzer, M. T. and Kleijn, C. R., 2013. "Benchmark numerical simulations of segmented two-phase flows in microchannels using the Volume of Fluid method", *Computers and Fluids*, 86, p. 28-36

Renardy, Y. and Renardy, M., 2002. "Prost: a parabolic reconstruction of surface tension for the volume-of-fluid method", *J. Comput. Phys.* 183, p. 400-421.

Sussman, M. and Puckett, E. G., 2000. "A coupled level set and volume-of-fluid method for computing 3D and axisymmetric incompressible two-phase flows", *Journal of Computational Physics*, 162, p. 301-337.

8. RESPONSIBILITY NOTICE

The authors are the only responsible for the printed material included in this paper.